2010 NDIA GROUND VEHICLE SYSTEMS ENGINEERING AND TECHNOLOGY SYMPOSIUM
MODELING & SIMULATION, TESTING AND VALIDATION (MSTV) MINI-SYMPOSIUM
AUGUST 17-19 DEARBORN, MICHIGAN

Development and Integration of a Soil-Tire Model for LAV-Terrain Systems

Xiong Zhang, PhD
Engineering Design & Development
General Dynamics Land Systems - Canada
London, Ontario

Zeljko Knezevic, M. Eng, MBA
Engineering Design & Development
General Dynamics Land Systems - Canada
London, Ontario

ABSTRACT

This paper presents a novel approach for modeling LAV-terrain systems in a dynamic simulation environment, which is based on results from the research and development of advanced technologies by the Computer Modeling and Simulation team of General Dynamics Land Systems-Canada (GDLS-C). The presented soil-tire model has been developed based upon the application of terra-mechanics and is being uniquely integrated with a full 8x8 LAV model in ADAMS/View, with incorporation of large tire deflections and multi-passing effect. It is shown that the highly efficient soil-tire model is capable of dynamically predicting soil sinkage, tire deflection, wheel slip, rolling resistance, drawbar pull and actual torque created at each soil-tire interface, as required by the mobility analysis of LAV systems over soft terrains.

INTRODUCTION

Predicting the performance of Light Armored Vehicle (LAV)-terrain systems in a dynamic virtual environment has remained a challenge over the past decade. The uncertainty of soil characteristics, the unavailability of reproducible terrain data and the manifold effects encountered at soil-tire interfaces, such as sinkage, multi-passing, slip and the elastic rebound of soil, make the modeling of LAV-terrain systems an extremely complicated and tedious process. However, given that the deformability of soil may significantly affect vehicle mobility, modeling soil-tire interactions is imperative in order to ensure the accuracy and reliability of simulation results.

The modeling of soil-tire interactions were based upon the knowledge of the physical processes invoked at soil-tire interfaces under different loading and terrain conditions. This necessitated the efforts conducted in experimental investigations [1-3] in support of the development of effective approaches to predict vehicle performance over soft terrains. Over the past decade, a variety of soil-tire models and their applications were reported by researchers considering different scenarios from different perspectives [4-15]. While significant progress has been made in modeling rigid wheel-soil interactions [7, 8, 10-13], there have been computer simulation models developed as independent software packages, such as AS^{2}TM by AESCO [9] and NWVPM by VSDC [16], for modeling both rigid wheel and elastic tire-soil interactions. Most of the reported models may be considered as application of the terra-mechanic principles developed from early studies [17-18] along with vehicle mobility analysis approaches detailed in [19]. It is noted that the majority of the reported soil-tire models assume small or rigid wheels, with their applications limited to mobile robotic platforms, planetary vehicles and other types of light off-road vehicle systems. Very few of the soil-tire models were reported to be integrated with commercial software to simulate heavy vehicle-terrain systems. Nevertheless, new versions of certain software start incorporating soil-tire models as its experimental features [20]. Efficient soil-tire programs for military vehicles with large deformable tires, although in high demand, have not yet been brought into a dynamic virtual environment as a mature product.

This paper presents a unique approach for modeling LAV-terrain systems in a dynamic simulation environment (ADAMS), with results showing the feasibility of predicting the mobility of LAVs over deformable terrains.

CONCERNS

There are a number of concerns that require attention in soil-tire model development as shown in Figure 1. One is due to the statistical scattering of soil characteristics. The

measurements are usually not reproducible, which may affect terrain parameter identification and model validation, especially when experimental means are not available or efficient. Another is due to the multiple effects of soil-tire interactions, such as soil sinkage, tire slip, soil rebounding, multi-passing, tire loads and tire kinematics, which are dynamically coupled together, making the modeling process extremely complicated, which may significantly affect the model efficiency and accuracy. The third one is the complexity of computing tire forces, requiring considerable amount of coding effort, especially when the limitations of software come into effect.

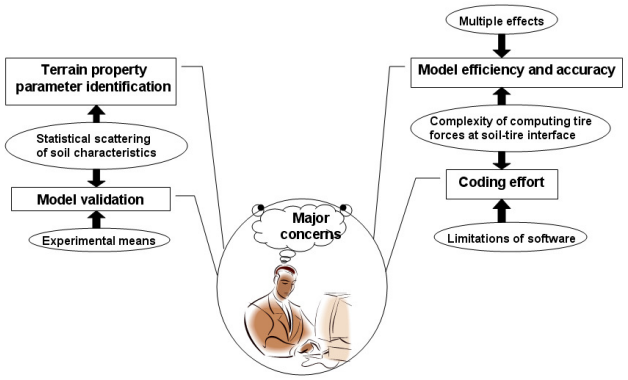

Figure 1: Concerns in soil-tire model development

The GDLS-C soil-tire (GDLS-C ST) model uses reported terrain data [19, 21] and the state-of-the-art approach to compute drawbar pull and other forces created at soil-tire interfaces, incorporating the multiple-effect of soil-tire interactions and multi-passing as well. Nevertheless, GDLS-C ST model was required to be integrated with ADAMS in support of mobility analysis of LAVs over soft terrains.

ASSUMPTIONS

Bekker's methodology [18] indicates that, at any point of soil-tire interface, the stress may be decomposed into two components, one acting normal to the interface, and the other acting in the tangential direction of the interface. In essence, the forces and the moment of forces about the tire center can be computed by integrating the stresses along soil-tire interface. This is the backbone of the GDLS-C soil tire model.

Figure 2 shows the assumptions for normal stress $p(\theta)$ and shear stress $\tau(\theta)$ distribution along an elastic tire-soil interface. It is assumed that both normal and shear stresses on the tire circumference along the soil-tire interface start from zero at point C (the point coming into contact with soil defined by angle θ_1) and increase in a linear manner (at different rates) as the point moving backward until it reaches point B (defined by angle θ_c), where the normal stress achieves its maximum value and remains constant throughout the flat portion AB, while the shear stress keeps increasing in a nonlinear manner along portion AB until it reaches its maximum value at point A (defined by angle $-\theta_c$). Both normal stress and shear stress decrease linearly to zero from point A to D along the AD portion of interface.

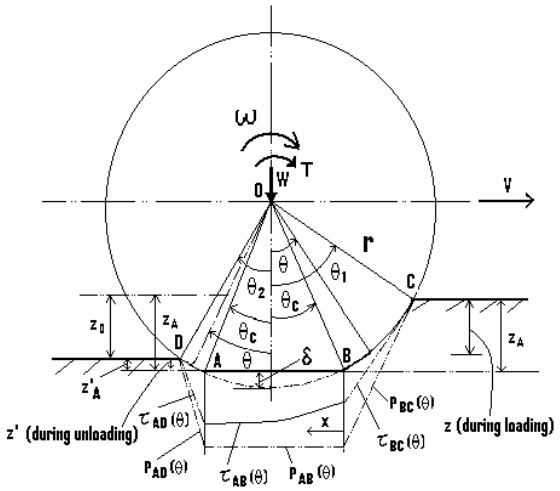

Figure 2: Illustration of GDLS-C ST model

Primary assumptions of the GDLS-C ST model include:

- Homogeneous terrain conditions
- Pressure-sinkage relationship characterized by [18]:
  - Soil sinkage modulus: K_c and K_Φ
  - Soil sinkage exponent: n
- Shear displacement-shear stress relationship [19]
- Tire force/torque equilibriums at each time instant

Additional assumptions of the GDLS-C ST model include:

- Constant wheel slip along flat portion AB
- Linear shear displacement along AB
- Constant normal stress along flat portion AB
- Liner normal stress distributions along BC and AD
- Liner shear stress distributions along BC and AD
- Variable tire inflation pressure depending on terrain

Homogeneous terrain conditions are required by the application of Bekker methodology [17-18]. The use of pressure-sinkage (p-s) and shear displacement - shear stress (sd-ss) relationships provides the chance of using a few number of parameters (k_1, k_2, n, etc.) to characterize terrain properties. Iterative numerical algorithms are developed to achieve force and torque equilibriums with the

use of monotonic functions. The core part of model development is the linearization of the stress distributions, except $\tau_{BC}(\theta)$, along each of the three portions of the soil-tire interface, namely, AD, AB and BC as shown in Figure 2. Definitions of symbols used by GDLS-C ST model are shown in Table 1.

Table 1: Symbols used by GDLS-C ST model

Symbols	Meaning of symbols
θ	Angular location of a point at soil-tire interface
θ_1	Front contact angle
θ_2	Rear contact angle
θ_c	Angular location of front/rear end of flat portion
z	Soil sinkage of a point at soil-tire interface
z_A	Maximum soil sinkage
$z_A^{'}$	Elastic rebound of soil
z_D	Unrecovered soil sinkage
$P_{AB}(\theta)$	Normal stress along AB as a function of θ
$P_{BC}(\theta)$	Normal stress along BC as a function of θ
$P_{AD}(\theta)$	Normal stress along AD as a function of θ
$\tau_{AB}(\theta)$	Shear stress along AB as a function of θ
$\tau_{BC}(\theta)$	Shear stress along BC as a function of θ
$\tau_{AD}(\theta)$	Shear stress along AD as a function of θ
k_c	Pressure sinkage modulus as defined in [19]
k_ϕ	Pressure sinkage modulus as defined in [19]
n	Soil sinkage exponent as defined in [19]
δ	Tire deflection
ω	Rotation speed of tire
W	Tire load
T	Torque applied by transmission line (per tire)
T_e	Effective torque created at soil-tire interface
V	Translational speed of tire at its center
b	Width of tire
r	Tire radius
x	Relative location of a point at flat portion AB

It should be mentioned that the GDLS-C ST model was required to model large tire subject to large load over deformable terrain and to be integrated with LAV models in ADAMS/View. The current model does not incorporate lateral tire dynamics, which may not be a major concern in most of the mobility analysis of LAVs.

FORMULATIONS

The general formulations used to compute the vertical force W, rolling resistance R, thrust F, drawbar pull DP and the effective torque T_e, are shown as follows.

Vertical force (tire load):

$$W = br\int_{\theta_c}^{\theta_1}\left[P_{BC}(\theta)\cos\theta + \tau_{BC}(\theta)\sin\theta\right]d\theta + br\int_{\theta_c}^{\theta_2}\left[P_{AD}(\theta)\cos\theta - \tau_{AD}(\theta)\sin\theta\right]d\theta + P_{AB}(\theta)bl_{AB} \quad (1)$$

Rolling resistance:

$$R = rb\left[\int_{\theta_c}^{\theta_1} P_{BC}(\theta)\sin\theta d\theta - \int_{\theta_c}^{\theta_2} P_{AD}(\theta)\sin\theta d\theta\right] \quad (2)$$

Thrust:

$$F = rb\left[\int_{\theta_c}^{\theta_1} \tau_{BC}(\theta)\cos\theta d\theta + \int_{\theta_c}^{\theta_2} \tau_{AD}(\theta)\cos\theta d\theta\right] + b\int_0^{l_{AB}} \tau_{AB}(x)dx \quad (3)$$

Drawbar pull

$$DP = F - R \quad (4)$$

Effective Torque:

$$T_e = br^2\left(\int_{\theta_c}^{\theta_1} \tau_{BC}(\theta)d\theta + \int_{\theta_c}^{\theta_2} \tau_{AD}(\theta)d\theta\right) + br\cos\theta_c\int_0^{l_{AB}} \tau_{AB}(x)dx \quad (5)$$

Given terrain and loading conditions, there are monotonic relationships existing distinctively between certain parameters, e.g., contact area vs. tire deflection at constant sinkage; contact area vs. sinkage at constant tire deflection; W or R vs. θ_1 under given tire loads. The observed monotonic relations could be taken as an advantage in the obtainment of numerical solutions as achieving force and torque equilibriums.

NUMERICAL ALGORITHIMS

Numerical algorithms (shown in Figure 3) were developed based upon the complete set of analytical equations derived (not shown), which characterize the features of the GDLS-C ST model. The numerical algorithms use iterative operations to achieve force and torque equilibriums. The force equilibrium means tire load is balanced by resultant soil reaction force (in vertical direction) plus the inertial force due to the bounce movement of tire. The torque equilibrium means the torque created at soil-tire interface (about tire center) is equal to driving torque (the torque applied by transmission line) plus the inertial torque due to the rotational movement of tire. In other words, both the vertical force equilibrium equation (V.F.E.E.) and the torque equilibrium equation (T.E.E.) have to be satisfied for a successful iterative operation loop as shown in Figure 3.

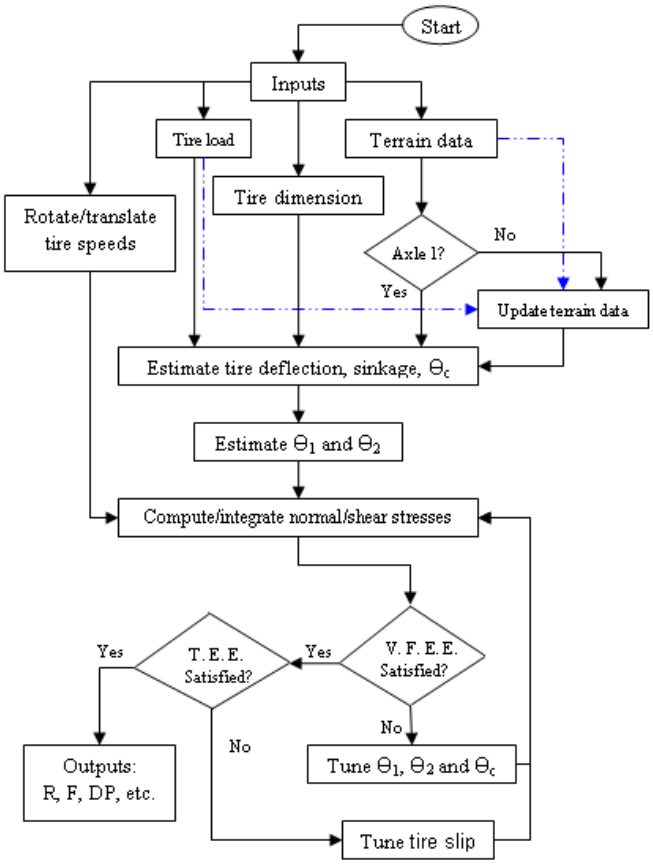

Figure 3: Flow chart of numerical algorithm used by GDLS-C ST model

The success of achieving converged solutions with iterative operations relies on the use of monotonic functions. The derivation and verification of the analytical monotonic functions appeared to be quite a tedious process, which has been completed with expected results.

As a common practice in calibrating empirical models, a number of scaling factors are introduced (not shown) to take account of the effect of tread pattern, differences between static data and dynamic calculations, etc, to ensure the obtainment of expected results. The application of scaling factors is further discussed as follows.

As an offset to Bekker's methodology, additional soil stiffness is introduced to modify the normal pressure calculation (based on p-s relationship), while a subprogram is used to estimate tire deflection as a function of inflation pressure, which is crucial in view of model efficiency. The model incorporates multi-passing effect by updating terrain property as a function of the tire load and sinkage recorded from preceding tire(s) and modifies the soil stiffness accordingly for subsequent tires.

The numerical algorithm was verified with a Matlab/Simulink program for a single tire-soil model under dry sand terrain conditions.

CHALLENGES

There are a number of challenges encountered yet resolved in the development and verification of the numerical algorithms for the GDLS-C ST model as outlined below.

Firstly, the flat portion assumed at soil-tire interface causes discontinuities in shear displacement and slip velocity, introducing additional complexity into the model and invoking extra cost in computing tire forces, making solving the problem more difficult.

Secondly, achieving force and torque equilibriums simultaneously appeared to be very challenging, which requires the development of numerical algorithms with consideration of multiple effects and the use of iterative operations. The observed monotonic functions are highly involved in resolving this challenge.

Thirdly, there is a contradiction between static and dynamics, noting that the soil parameters were derived based upon measurements from static tests (p-s relationship), or steady-state tests (sd-ss relationship), while the interactions at soil-tire interface is actually of transient or dynamic nature. Although this issue may affect the accuracy of the results, it does not affect the running of the computing process. Complete resolution of this issue relies on the use of experimental means and the outcomes from model validation effort, which is a part of future work.

Lastly, modeling the multi-passing effect requires the repetitive use of modified single tire-soil model, with consideration of the sequence of the wheel and the specific loading-unloading-reloading cycle for each wheel, adding more complexities into the modeling process. Note the soil rebounding property can be obtained by conducting soil

Approved for Public Release, Distribution Unlimited, GDLS approved, Log No. 2010-77, dated 07/13/10

rebounding tests, while accurate modeling of elastic rebound require sufficient soil measurements.

The above mentioned challenges have been resolved by using either analytical solution of the related mathematical model or numerical techniques, as well as a number of scaling factors introduced by trial and error method.

MODEL INTEGRATION

With success in the verification of the numerical algorithms for single tire-soil model, we come to the point of bringing the soft-soil tire model into the dynamic simulation environment of ADAMS.

By using ADAMS/Controls, the model integration starts with connecting the soil-tire program in Simulink with a single-wheel model in ADAMS/View, followed by the integration of two-wheel and four-wheel models.

Single-Wheel Model Integration

The architecture of integrating the soil-tire module with a single-wheel ADAMS model (ADAMS plant exported from ADAMS/View and imported to Simulink) is illustrated in Figure 4.

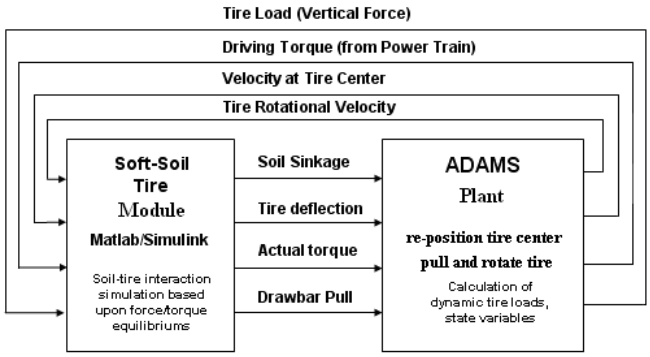

Figure 4: Integration architecture for single-wheel model

The single tire-soil module in Simulink calculates and outputs soil sinkage, tire deflection, actual torque and drawbar pull (to ADAMS plant), which are used by the ADAMS model to update tire center position and calculate state variables in terms of tire velocities and dynamic tire loads, which are then fed back to the soil-tire module for the next iteration. The iterative process continues until the simulation is completed.

Figure 5 shows the single-wheel model in ADAMS/View linked with the soil-tire module in Simulink. The upper block represents sprung mass, while the lower block represents the wheel hub. The upper spring models suspension stiffness. The blue horizontal line represents the top surface of un-deformed ground, while the purple line represents the instantaneous position of the top surface of deformed soil (underneath tire center) at each time instant. The difference between the blue line and purple line illustrates soil sinkage, while the distance between the lowest point of tire and the purple line shows tire deflection.

Note that the general forces acting at tire center, including the torque rotating the wheel and the drawbar pull pulling the wheel moving ahead, are all computed by the soil-tire interaction program in Simulink, with the original ADAMS/Tire solver replaced by the soil-tire module.

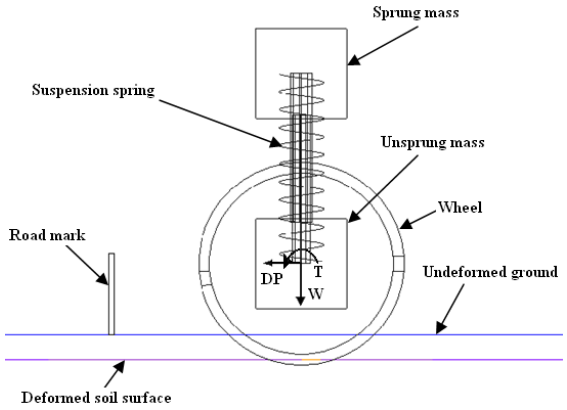

Figure 5: Single-wheel model in ADAMS/View

Two-Wheel Model Integration

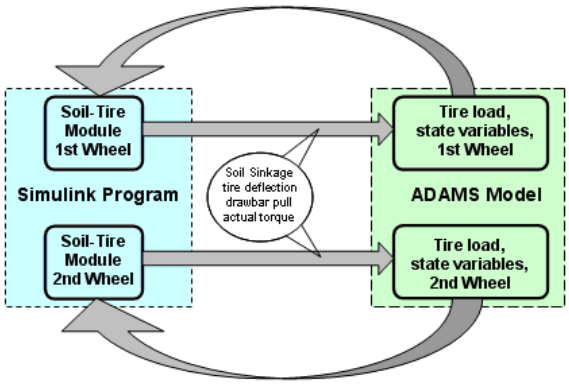

Figure 6: Integration architecture for two-wheel model

With success in the integration of single-wheel model, the soil-tire module was then integrated with a two-wheel model in ADAMS/View, with incorporation of multi-passing

effects. The integration architecture for two-wheel model is illustrated in Figure 6.

Integration of the soil-tire module with the two-wheel model is similar to that for single-wheel model except that the iterative process circulates for individual wheel separately. The two-wheel ADAMS model calculates all the state variables required as the inputs to both wheels at each iterative step. The iterative process continues until the simulation is completed. Figure 7 shows the two-wheel model in ADAMS/View linked with two tire-soil module in Simulink. Similar to the single-wheel model, the lower blocks represent wheel hubs, while the upper blocks represent sprung mass over each wheel. The upper springs model the suspension stiffness over two wheels. The sprung mass and suspension stiffness for the first and second wheel are set different to investigate the performance of soil-tire algorithm under different loads. The two sprung masses are linked by two beams connected through translational joints and a spring element to simulate the force transmission between two axles. The blue horizontal line represents the original un-deformed ground, while purple line and grey line represent the top surfaces of deformed soils under each wheel, showing the soil sinkage and tire deflection for each wheel at each time instant. In addition, the position of first tire center is determined by the soil-sinkage and tire deflection invoked by the first wheel, while the position of second tire center is determined by the soil-sinkage and tire deflection invoked by the second wheel, and the soil sinkage induced by first wheel. Again, the tires are driven by the forces computed by soft-soil tire modules in Simulink.

Four-Wheel Model Integration

Figure 8 illustrates the integration architecture for the four-wheel model, which is similar to that for two-wheel model except that the iterative process circulates for each of the four wheels (other than two wheels) separately. Nevertheless, the Adams model calculates all the state variables required by each of the four wheels at each iterative step. The iterative process continues until the simulation is completed.

Figure 9 shows the four-wheel model in ADAMS/View linked with four soil-tire modules in Simulink. Similar to the two-wheel model, the lower blocks represent wheel hubs, while the upper blocks represent sprung mass over each wheel. The upper springs model the suspension stiffness over four wheels. Unlike the two-wheel model, the sprung mass and suspension stiffness over each wheel are set as the same for all the wheels to investigate the performance of the soil-tire model in view of repetitive loading effect under similar axle loads. Similar to the two-wheel model, the position of the following tire center is determined with consideration of the soil-sinkage invoked by preceding wheel(s).

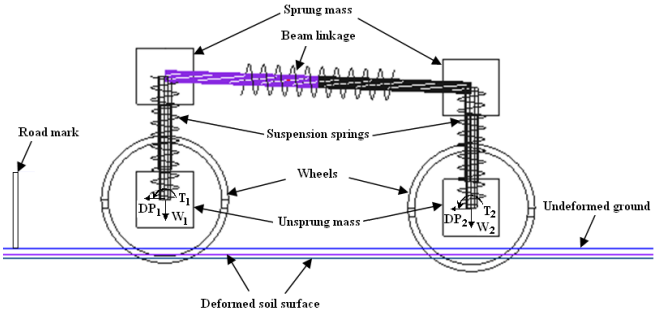

Figure 7: Two-wheel model in ADAMS/View

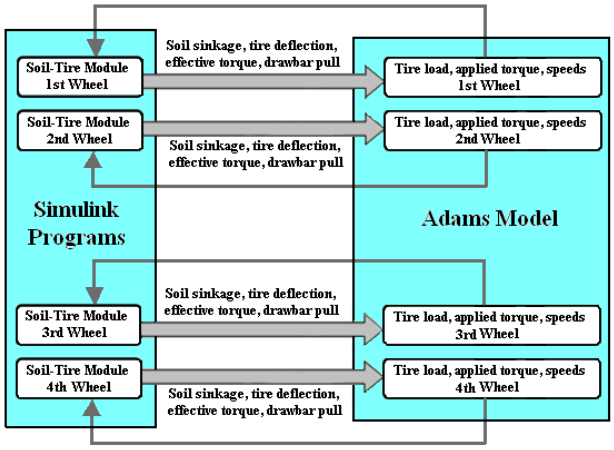

Figure 8: Integration architecture for four-wheel model

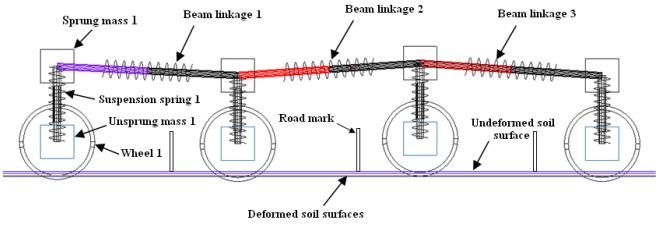

Figure 9: Four-wheel model in ADAMS/View

Figure 10 further shows the Simulink program for the four-wheel model. The adams_sub block represents the ADAMS plant of the four-wheel model shown in Figure 9. The inputs to the ADAMS plant come from four Demux blocks that correspond to four wheels. Each Demux block includes the updated soil sinkage, tire deflection, drawbar pull and effective torque computed by corresponding soil-tire module program. The outputs from ADAMS plant are grouped by four Mux blocks connected to four wheels. Each Mux block

outputs the updated tire load and tire speeds computed by ADAMS plant, to the soil-tire programs associated with each corresponding wheel.

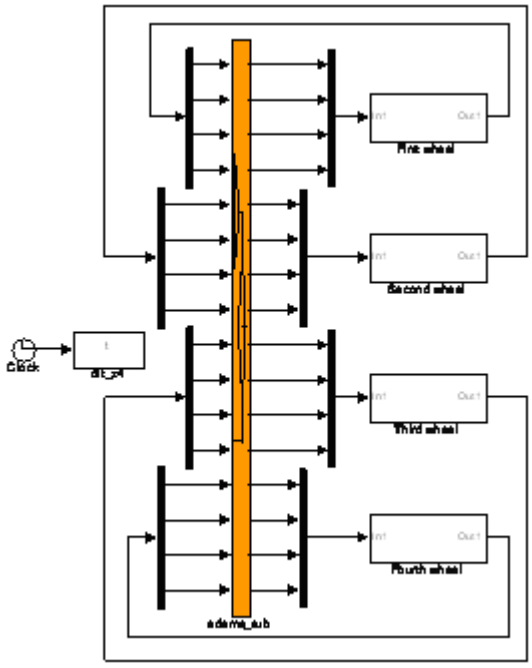

Figure 10: Simulink program for four-wheel model

Full-Vehicle Model Integration

With the soil-tire module verified with the single-wheel, two-wheel and four-wheel models, a full 8x8 LAV model in ADAMS/View (shown in Figure 11) is used to further verify the feasibility of replacing the ADAMS/Tire solver with the GDLS-C ST module. The numerical results from the full LAV model are discussed in the next section.

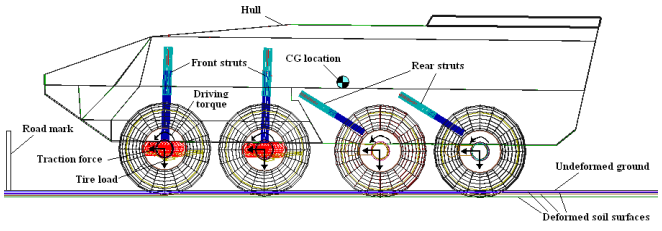

Figure 11: A full 8x8 LAV model in ADAMS/View

SIMULATION OF A FULL 8x8 LAV MODEL

Inputs for Simulation

A mission profile for a LAV typically consists of a variety of highly deformable terrains, which may range from desert sands through soft mud to fresh snow. The GDLS-C ST model is expected to function well with the terrains shown in most of the mission profiles. With this in mind, two typical terrains (lean clay and dry sand) and three vehicle weights (24klbs, 28klbs and 32klbs) are used in the simulation to derive the results showing the performance of the GDLS-C ST model as integrated with full LAV models in ADAMS.

The terrain parameters used in the simulation are chosen from reported study [19] and listed in Table 2. Note the method of estimation of terrain parameters can be found in thesis work by Kang [21].

Table 2: Considered terrain parameters

Terrain	n	K_c (kN/m^{n+1})	K_Φ (kN/m^{n+2})	C (kPa)	Φ (deg)
Dry sand	1.1	0.99	1528.43	1.04	28
Lean clay	0.2	16.43	1724.69	68.95	20

Figure 12 shows the driving torque applied at each wheel in a simulation of a full LAV model over lean clay terrain. The stepped torque inputs are used to show the performance of the soil-tire model under varying torque inputs. The maximum magnitude of torque (constant after 28s) is selected to match the minimum torque required for the same LAV model to steadily move up a 10degree slope on a highway road. Under dry sand conditions, the maximum magnitude of torque is selected to match the minimum torque required for the same LAV model to steadily move up a steeper slope (17degree slope on highway road). The driving torque applied for each simulation is proportional to gross vehicle weight (GVW) in order to evaluate the mobility characteristics of the LAV model with different weights over the two selected terrains. The tire inflation pressure over lean clay terrain is set considerably higher than that under dry sand conditions.

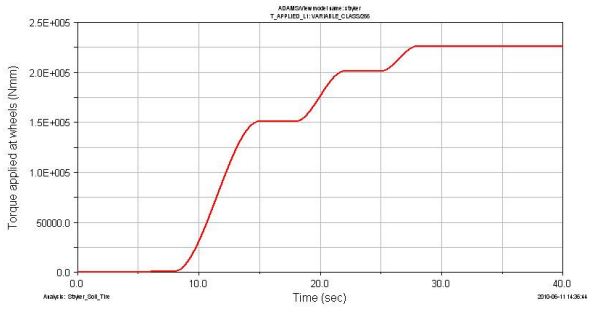

Figure 12: Driving torque used in a simulation (lean clay)

Note that the application of a small (negligible) magnitude of driving torque with sufficient long time (4s), which is not clearly shown in Figure 12, allows a smooth transition for the soil-tire module to switch from "settling" to "traction" phase, namely, switching from subprogram for settling due to gravity effect to subprogram for traction process.

Results from Simulation

With the driving torque proportional to vehicle weight, simulation results were obtained to show the mobility characteristics of the LAV model in terms of the drawbar pull as a function of vehicle weight and terrain property.

Figure 13 shows the drawbar pull (per tire on left side) computed from the LAV model (GVW=28klbs) over lean clay terrain. Due to the differences in tire loads and soil-tire contact geometry, the net horizontal force or drawbar pull computed for each soil-tire interface appears to be quite different, which takes a negative value when the resistance is greater than the thrust. This is especially true at the initial application of the driving torque (as shown in Figure 13). In simulations, the vehicle model starts moving ahead when the total drawbar pull (of the entire vehicle) is greater than zero. Note that Figure 13 shows only the drawbar pull (per tire) after the vehicle model starts moving.

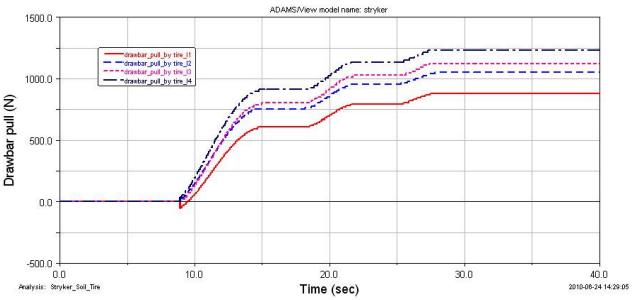

Figure 13: Drawbar pull per tire as a function of time (28klbs model, lean clay)

Similar to drawbar pull (per tire), the effective torques computed for each wheel appear to be different in magnitudes, resulting in different spinning speeds for different wheels (not shown). Figure 14 shows the translational speed at tire center and the product of rotational speed of tire and its effective radius for first axle of the LAV model with 28klbs weight over lean clay terrain.

Figure 15 through 18 further illustrate the simulation results, in terms of the ratio of drawbar pull over vehicle weight (DP/GVW), vehicle speed at 32s (32s after the application of driving torques, which corresponds to 40s in simulation), drawbar pull (DP) of entire vehicle, and the averaged soil-sinkage and tire deflection, as a function of GVW under lean clay and dry sand terrain conditions.

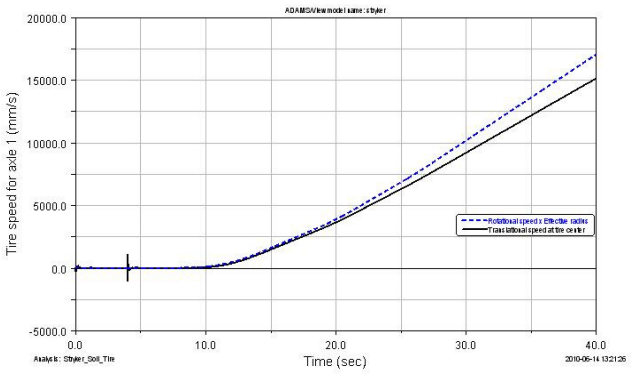

Figure 14: Tire speeds as a function of time (28klbs model over lean clay)

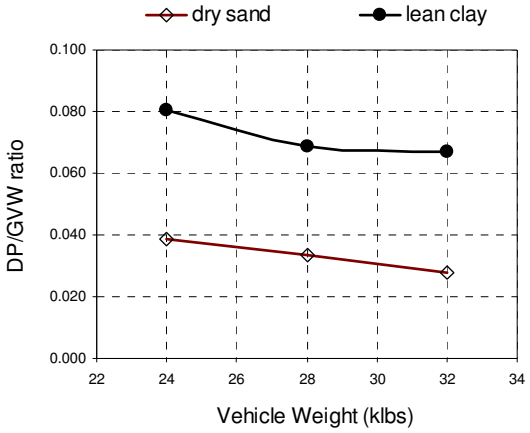

Figure 15: DP/GVW ratio as a function of GVW

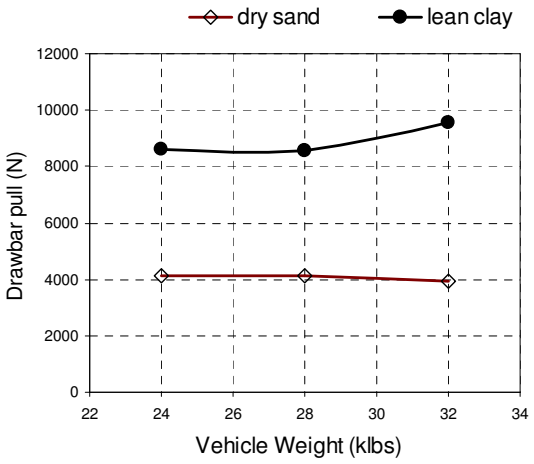

Figure 16: Drawbar pull as a function of GVW

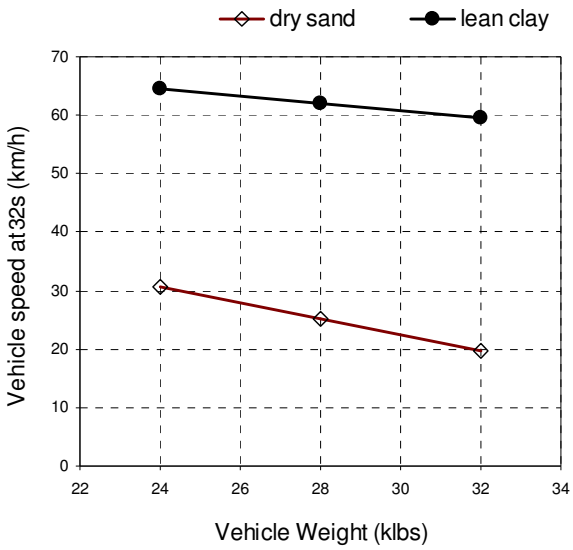

Figure 17: Vehicle speeds at 32s as a function of GVW

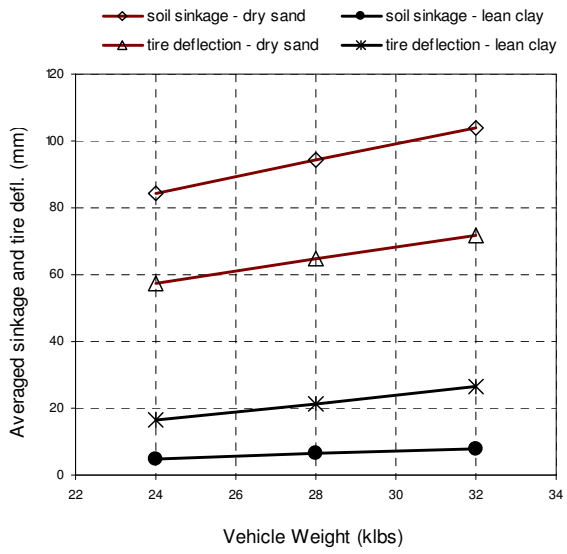

Figure 18: Averaged soil-sinkage and tire deflection as a function of GVW

It is observed that larger wheel slips (10-20%) occur at soil-tire interfaces, in comparison to those at tire-road contact patches, which is normally under 10%. Figure 15 shows that the vehicle mobility degraded as vehicle's weight increased from 24klbs to 32klbs under dry sand condition. Under lean clay conditions, however, the vehicle's mobility dropped considerably as vehicle weight increased from 24klbs to 28klbs yet only slightly degrading as the vehicle weight increased further (from 28klbs to 32klbs). This may be contributed to the increased length of the flat portion of the soil-tire interface, which enlarged the traction force and tends to maintain the mobility level as tire load increases. Figure 16 shows that under dry sand conditions, the drawbar pull does not change as vehicle weight increases from 24klbs to 28klbs and slightly decreases with the increase in vehicle weight from 28klbs to 32klbs, resulting in considerable degrading of mobility. Under lean clay conditions, the drawbar pull decreased slightly as vehicle weight increased from 24klbs to 28klbs and then increased considerably with further increase (from 28klbs to 32klbs) in vehicle weight. These observations are consistent with the results shown in Figure 15. Figure 17 further confirms that the heavier the vehicle weight, the greater the loss in mobility in terms of vehicle speed (at 32s). Keep in mind that the applied driving torques are proportional to the vehicle weight and the maximum driving torques are equivalent to the minimum torque required for the same vehicle to climb up 10degree and 17degree longitudinal slope under lean clay and dry sand conditions, respectively.

The averaged soil sinkage and tire deflection increased with increase in vehicle weight, as shown in Figure 18. Note that under dry sand conditions, the tire inflation pressure has to be quite low to ensure sufficiently large flat portion of soil-tire interface such that drawbar pull can be generated to a full extent. This results in larger tire deflection under dry sand conditions than that over lean clay terrain.

Note that there is no test data to correlate to the model. The simulation results presented in this section are thus not intended for quantitative analysis but for the demonstration of the feasibility of replacing ADAMS/Tire solver with the GDLS-C ST model, and the capability of predicting the mobility characteristics of LAVs over deformable terrains in a qualitative manner.

Conclusions

Based upon the application of terra-mechanics, an efficient soil-tire model has been developed and successfully integrated with models in ADAMS. The feasibility of using the GDLS-C ST model to simulate a LAV-terrain system has been demonstrated. The approach of model integration is unique and potentially applicable to any efficient soil-tire models. The results from this study provide an access to predict the mobility of LAV systems in a dynamic environment, and a connection between a highly efficient analytical soil-tire model and the commercial software being used by military vehicle manufactures.

The data presented are not intended for quantitative analysis. The simulation results from the full LAV model considered, however, reveal the effect of vehicle weight and terrain properties on vehicle mobility, highlighting the potential application of the GDLS-C ST model in mobility analysis of LAV systems over deformable terrains.

Future Work

Future work includes validation of model results and model parameters with test data as well as incorporation of lateral vehicle dynamics.

REFERENCES

[1] Leslie L. Karafiath, "Soil-tire model for the analysis of off-road tire performance", Pentagon report, report number: 0174247, research memo, 34 pages, May 1972.

[2] Eddie C. Burt, Alvin C. Bailey and Randall K. Wood, "Effects of soil and operational parameters on soil-tire interface stress vectors", International journal of Terramechanics, vol. 24, Issue 3, pages 235-246, 1987.

[3] S. K. Upadhyaya and D. Wulfsohn, "Traction prediction using soil parameters obtained with an instrumented analog device", International journal of Terramechanics, vol. 30, Issue 2, pages 85-100, March 1993.

[4] F. R. Fassbender, C. W. Fervers, C. Harnisch, "Approaches to predict the vehicle dynamics on soft soil", Vehicle System Dynamics, vol. 27, Issue S1, pages 173 – 188, 1997

[5] M. Saarilahti, "Soil Interaction Model", ECOWOOD studies made at the University of Helsinki, University of Helsinki, Department of Forest Resource Management, Publications 31, ISBN 951-45-9087-2. ISSN 1236-1313. Helsinki 2003.

[6] P. Defossez, and G. Richard, "Models of soil compaction due to traffic and their evaluation", International journal of Soil & Tillage Research, vol. 67, Issue 1, pages 41-64, August 2002.

[7] K. Iagnemma and K. Shibly, "On-Line Terrain Parameter Estimation for Planetary Rovers", Proc. of the 2002 IEEE International Conference on Robotics and Automation, Washington, DC, pages 3142-3147.

[8] M. Gysi, V. Maeder, P. Weisskopf, "Pressure distribution underneath tires of agricultural vehicles", Transactions of the ASABE, Vol. 44(6): pages 1385–1389, 2001.

[9] AESCO, "AS2TM User's Guide", version 1.03, 2006.

[10] K. Iagnemma, S. Kang, H. Shibly, and S. Dubowsky, "On-Line Terrain Parameter Estimation for Planetary Rovers", IEEE Transactions on Robotics, Vol. 20, No. 5, pp. 921-927, October, 2004.

[11] H. Shibly, K. Iagnemma, S. Dubowsky, "An equivalent Soil Mechanics Formulation for Rigid Wheels in Deformable Terrain, with application to Planetary Exploration Rovers", Journal of Terra-mechanics 42, pp. 1-13, 2005.

[12] G. Ishigami, A. Miwa, K. Nagatani, K. Yoshida, "Terramechanics-Based Model for Steering Maneuver of Planetary Exploration Rovers on Loose Soil", Journal of Field robotics 24(3), pp., 233-250, 2007, Wiley Periodicals, Inc.

[13] G. Ishigami, "Terramechanics-based Analysis and Control for Lunar/Planetary Exploration Robots", doctoral dissertation, Department of Aerospace Engineering, Tohoku University, Japan, 2008.

[14] C. Harnisch, B. Lach, R. Jakobs, M Troulis, and O. Nehls, "A new tyre-soil interaction model for vehicle simulation on deformable ground", International Journal of Vehicle System Dynamics, Vol. 43, Issue 1, Supplement 1, pp. 384 - 394, 2005.

[15] J. Y. Wong, "Terramechanics and Off-Road Vehicle Engineering: Terrain Behaviour, Off-Road Vehicle Performance and Design", 2nd edition, Butterworth-Heinemann, Elsevier 2010.

[16] "Computer Simulation Models for Design and Performance Evaluation of Off-Road Vehicles", Vehicle Systems Development Corporation (VSDC), Ottawa, Ontario, 2009.

[17] J.Y. Wong and A.R. Reece, "Prediction of Rigid Wheel Performance Based on the Analysis of Soil-wheel Stresses Part I. Performance of Driven Rigid Wheels", J. Terramechanics, Vol. 4, No. 1, 81–98, 1967.

[18] M. G. Bekker, "Introduction to Terrain-Vehicle Systems", Ann Arbor, University of Michigan Press, 1969.

[19] J. Y. Wong, "Theory of Ground Vehicles", 4th edition, John Wiley, New York, 2008.

[20] MD-Adams-2010-Release-Guide.

[21] S. Kang, "Terrain Parameter Estimation and Traversability Assessment for Mobile Robots", master thesis, Massachusetts Institute of Technology May 2003.